Directional Spectra of Seas near Full Development

J. A. EWING AND A. K. LAING*

Institute of Oceanographic Sciences, Wormley, Surrey GU8 5UB, England

(Manuscript received 8 September 1986, in final form 28 April 1987)

ABSTRACT

Estimates of the directional wave spectrum have been obtained from a data buoy in the southwest approaches to the British Isles. Four years of simultaneous wave and wind data measured at the data buoy were screened for conditions approaching full development. The observed frequency spectra were made nondimensional using the similarity law of Kitaigorodskii and then averaged over six wind speed classes. Comparisons are made with the Pierson–Moskowitz spectrum for fully developed seas. For wind speeds (at the 10 m level) below 16 m s^{-1}, the averaged spectrum lies consistently below the Pierson–Moskowitz form, while for higher wind speeds the spectra in the region of the peak have similar values to this spectrum. Similarly, values of the nondimensional wave energy are significantly lower than the Pierson–Moskowitz value for wind speeds less than 16 m s^{-1}. For higher wind speeds, the nondimensional wave energy is close to the Pierson–Moskowitz value. The directional spread was studied using two parameters derived from the first- and second-order harmonics of the angular distribution. The spread parameter s_2, which depends on the second-order harmonics, was found to be more reliable. Estimates of s_2 as a function of wave frequency in relation to peak frequency differ from the expression for fetch-limited waves. Although the peak value is comparable, the decrease with increasing frequency is less rapid.

1. Introduction

One of the most important contributions to the study of ocean waves has been the work of Pierson and Moskowitz (1964) in the formulation of a spectral form for fully developed seas. These authors studied the synoptic weather maps from 1955 to 1960 to identify such conditions, which then could be associated with measurements taken on weather ships in the North Atlantic Ocean. From an analysis of over 400 wave records, Pierson and Moskowitz obtained a subset of about 50 wave spectra that satisfied their criteria for fully developed conditions. Finally, they derived a spectral form which fitted the observed wave spectra and also obeyed the similarity laws proposed by Kitaigorodskii (1962).

In recent years oceanographers have paid particular attention to the study of fetch-limited waves. The pioneering work of the Joint North Sea Wave Project (Hasselmann et al., 1973) identified the principal source terms governing the evolution of the wave spectrum. However, the transition from limited fetch to fully developed conditions is not attainable in such studies since the wind is seldom steady enough to produce a fully developed state and the fetch is always limited in extent. The approach to a fully developed state can be understood qualitatively in terms of the source terms. Nonlinear interactions transfer energy to lower frequencies so that the peak frequency decreases with fetch. At the same time, the growth of waves directly from the wind decreases as the phase speed of the most energetic waves approaches the wind speed. The high-frequency part of the wave spectrum becomes independent of fetch due to the balance of source terms in this region.

Komen et al. (1984) have recently considered the energy balance in fully developed sea states by direct integration of the transport equation with specified source terms. They showed that the Pierson–Moskowitz (hereafter P–M) form was close to their best solution for an asymptotic fully developed state. However, these authors also found that the associated directional distribution did not conform to existing ideas of the spreading function (Hasselmann et al., 1980). In particular the directional distribution was most narrow at a frequency above the spectral peak and comparatively broad at the spectral peak.

The purpose of this paper is to consider the form of the frequency spectrum and its directional characteristics for conditions approaching full development using a long series of wave and wind measurements obtained from a data buoy in the southwest approaches to the British Isles. Directional wave spectra measurements from this data buoy, DB1, have been collected by the U.K. Offshore Operators Association over a period from June 1978 to March 1982.

The outline of the paper is as follows. We first describe the data buoy and its measurement system. Then we discuss the selection of records corresponding to

* Permanent address: New Zealand Meteorological Service, P.O. Box 722, Wellington 1, New Zealand.

fully developed events by considering the time history of the winds and the characteristics of the directional spectrum. The frequency spectrum is then studied and comparisons are made with the P–M form. Finally, we consider the form of the directional distribution.

2. Data buoy measurements

The data buoy DB1 was moored at a position 48°43′N, 8°58′W in a depth of water of 170 m (Fig. 1). The buoy had a diameter of 7.6 m and in addition to the wave sensors was equipped with sensors to measure wind speed and direction, surface currents and air and sea temperature (Fig. 2). A full description of the data buoy is given by Freathy et al. (1982). (DB1 was replaced by another buoy in 1984.)

Wave measurements were obtained from a Datawell Hippy 40-sec sensor near the center of gravity of the buoy. This sensor measures the heave acceleration together with pitch and roll of the buoy. The heave acceleration was converted to displacement by electronic double integration. Heave displacement, pitch, and roll were then sampled simultaneously, together with a compass reading to give the buoy heading, at 1.2 sec intervals. The length of each wave recording was 20 min.

Comparisons of results from DB1 against an IOS pitch–roll buoy of 1.2-m diameter indicate that valid results were obtained from the larger buoy up to a frequency of 0.20 Hz (Clayson and Ewing, 1977). For this value of wave frequency, the ratio of buoy diameter to wavelength is 5.1. Using the theory of Kim (1966) for a ⅛ ellipsoid, we obtain a heave amplitude response of 0.95 at this wave frequency. We therefore adopt a wave frequency of 0.20 Hz for the limit of validity of our results.

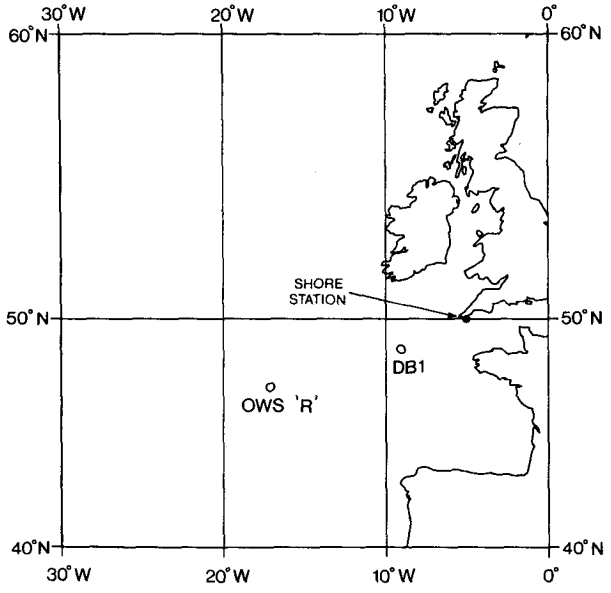

FIG. 1. Location of data buoy DB1 and Ocean Weather Ship Romeo.

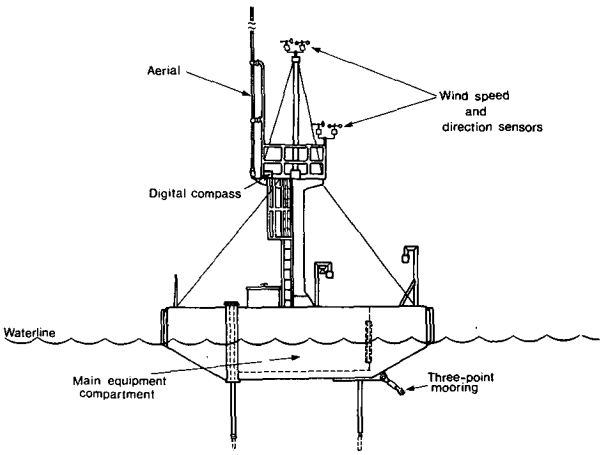

FIG. 2. Schematic diagram showing wave and wind sensors on data buoy DB1.

Wind speed and direction were obtained from a standard cup anemometer and vane mounted at two positions with heights 6.0 and 8.7 m above the sea surface. The mean wind speed and direction were then derived from an average over a 10-min interval.

The meteorological data were measured for the last 10 min of every hour and transmitted by radio to a nearby shore station where the data were sent by land line to the laboratory at EMI, Woking. (The Meteorological Office had access to the hourly reports in real time.) The wave data, consisting of time series of heave, pitch, roll and buoy heading, were measured every 3 h, starting on the hour, and were also transmitted to the shore station. To safeguard against loss of data due to radio transmission difficulties, the hourly reports and the heave time series were stored on a high-density cassette recorder on the buoy. Finally, the recorded and transmitted data were quality checked and then merged ready for analysis.

3. Analysis

The determination of the directional spectrum follows the classical method first suggested in Longuet-Higgins et al. (1963) and Cartwright (1963). The pitch, roll and compass channels are used to derive the two components of surface slope with respect to N–E axes. The heave displacement and surface slopes are then used to estimate the relevant cross spectra using an implementation of the Fast Fourier Transform algorithm due to R. C. Singleton of the Stanford Research Institute. The cross spectra were formed from ensemble averages of the computed spectra over 11 nonoverlapping sections each of length 100 s. This procedure yields spectral estimates at a resolution of 0.01 Hz with 22 degrees of freedom. The analysis is summarized in the Appendix.

The principal parameters we shall use from this analysis are the frequency spectrum E, the mean wave direction θ_1 and the directional spread parameters s_1 and s_2. All these parameters are functions of the wave frequency f (in Hertz).

All the meteorological and oceanographic data from DB1 are stored on magnetic tape in the data bank of the Marine Information Advisory Service at IOS, Bidston.

4. Selection of records for fully developed conditions

The selection of fully developed events needs particular care. Given that the nature of the conditions under study require that the measurements are made in the open ocean where geographical boundaries do not limit wave growth, it is difficult to ensure that the measurements are not influenced by swell, upwind variations in fetch conditions, or that the waves have in fact reached a steady state of development. Ideally, we require measurements of the wind field for about eight hours and over about 500 km upwind of DB1. Such information is not available and we therefore have to use a single point measurement of the wind speed.

In such conditions, meteorological data alone are insufficient to determine fully developed conditions and we need to use the spectra from our wave measurements to aid the screening process. We require events in which the spectrum is stationary over a long period, the wind speed and direction are likewise steady at the site and in the generating area, and the spectrum has reached a level consistent with maximum development for the wind speed.

The event selection was made in several stages. First, the 3-h wave records were screened using a number of criteria based on parameters of the frequency spectrum and the wind speed. From these records events were selected from persistent, near-stationary sequences. These were then screened to ensure that the directional characteristics of wind and waves were consistent. Finally, the events were checked against meteorological information from a much wider area.

For the first step, a conventional JONSWAP spectrum was fitted to each 3-h spectrum to give the peak frequency f_m, the peak enhancement factor γ and the equilibrium range parameter α. The method of fitting followed the procedure given by Muller (1976) using the frequency spectrum estimated at 0.01 Hz intervals. Estimates of the JONSWAP parameters are made over the range from $1.35f_m$ to $2f_m$, or 0.2 Hz, whichever is the least. The significant wave height, h_s, was calculated from the area under the wave spectrum up to a frequency of 0.20 Hz. This results in at most a 5% underestimation. A mean wind speed representative of each 3-h period was calculated for a 7.2-m level (the geometric mean height of the two anemometers) by averaging the six values available (three hourly values at each of two levels). To adjust this to a 10-m level a neutrally stable profile was used with drag coefficient, C_D, given by Wu (1982). That is,

$$U(z)/U_{10} = 1 + \frac{\sqrt{C_D}}{\kappa} \ln\left(\frac{z}{10}\right)$$

where $C_D = (0.8 + 0.065U_{10}) \times 10^{-3}$, κ is von Karman's constant (0.41), and $z = 7.2$ m. U_{10} is in m s^{-1}.

The fully developed state is reached when, for a given steady wind speed, the total variance ceases to increase. This is accompanied by a halt in the downshift of the peak frequency such that $\nu = U_{10}f_m/g$ reaches approximately 0.13: the ratio of the wind speed to phase velocity is then 0.82. Reanalysis of the Pierson–Moskowitz data (1964) using the JONSWAP shape (see Hasselmann et al., 1976) has revealed that values of γ of about 1.4 are appropriate for fully developed conditions; larger values of γ are associated with developing seas. For a given wind speed the P–M spectrum allows us to calculate a significant wave height, h_{PM}. With these values, and the conventions previously outlined, the following test was devised:

(a) $0.11 < \nu < 0.18$
(b) $0.7 < \gamma < 2.5$
(c) $h_s > 1$ m
(d) $h_s < 1.5h_{PM}$
(e) $U_{10} > 5$ m s^{-1}.

Low values of γ and ν usually indicate the presence of swell and possibly multiple peaks in the frequency spectrum. Values of significant wave height exceeding h_{PM} also indicate the presence of swell. Reasonably wide margins have been used to allow for the sensitivity of these parameters to small errors in the wind speed.

Using this test a list of wave records was drawn from the available data. These were then scanned for sets of three or more contiguous records which satisfied the following additional constraints:

(i) 3-h wind speeds did not vary more than 10% and were not decreasing
(ii) wind direction did not vary more than 30°
(iii) significant wave height varied less than 15%.

As a result of the above procedure, 45 events were identified. A directional analysis of these wave data was then performed and a graphical display made of the frequency spectrum, the check ratio R, the mean wave direction and the directional spread parameters s_1 and s_2, all as functions of frequency. For most records the check ratio R (see Appendix) was near unity close to the spectral peak, but reached values of approximately 1.2 at higher frequencies. We consider that the tilt of the buoy is reduced at higher frequencies due to the three-point mooring, with the result that R is increased to values greater than unity. This enabled us to check that the mean wave direction did not vary more than 30° from the wind direction and did not vary over the frequency range (another possible indi-

cation of the presence of swell or veering wind). The frequency spectrum was also checked for bimodality which could not reasonably be explained by the sampling variability associated with 22 degrees of freedom in the spectral estimates. These checks were failed by 12 events. Finally, 33 events were accepted as being representative of fully developed conditions.

Using the final three of the 3-hourly wave records for each satisfactory sequence, mean cross spectra were calculated for each event; this can be regarded as being representative of a 9-h period with 66 degrees of freedom. The frequency and directional characteristics were recalculated for these spectra and they were checked in the same manner as the individual 3-h spectra. Two examples of 9-h spectra are shown in Fig. 3a, b. The former is a good example of the type of event we have been seeking; the latter is a marginal case where wind direction and wave direction show some discrepancy and the wave direction varies with frequency. Characteristics of the 9-h spectra for these events, including the JONSWAP parameters, are given in Table 1. Some of the records had invalid directional data due to gaps in the slope records caused by radio transmission faults. These events were not used in the directional analysis. However, the heave records were complete and all frequency analyses were included.

Finally, the charts from the Daily Weather Summaries, produced by the Meteorological Office, were inspected for a period of two days preceding each of the selected events. Although an occasional minor front passed through the generation area for waves arriving at DB1 during these events, in all cases the changes in wind speed and direction accompanying these fronts were insubstantial and transient. Further, in very few cases was there any substantial change in the orientation of the fetch during the whole two-day period prior to the selected records. Table 1 includes an identification "*f*" for a weak front which passed through the fetch sometime during the preceding two days, and "*d*," indicating that a directional variation of more than 45° occurred somewhere in the fetch. For winds from the southwest to the northwest, Ocean Weather Ship Romeo at position 47°N, 17°W (see Fig. 1) was suitably placed to provide observations 610 km upwind in the fetch. Table 2 shows several examples of the wind history at OWS R for a period up to 18 h preceding the time T a wave at the peak frequency would have to pass OWS R to reach DB1 during one of the recorded events. Also included are the mean wind speed and direction for the 9-h event at DB1.

5. The frequency spectra

a. Similarity theory

The similarity theory and dimensional analysis of Kitaigorodskii (1973, Chap. 6) provide a framework within which it is possible to study the spectral form of fully developed waves. In the fully developed state, the spectrum E, when scaled with U_∞ and g, must be a function of $U_\infty f/g$, that is,

$$E(f)g^3/U_\infty{}^5 = H(U_\infty f/g).$$

Here U_∞ is the mean wind speed at the top of the surface boundary layer. At this level the mean wind speed should not be influenced by energy transfer from the atmosphere to the waves. Following the work in

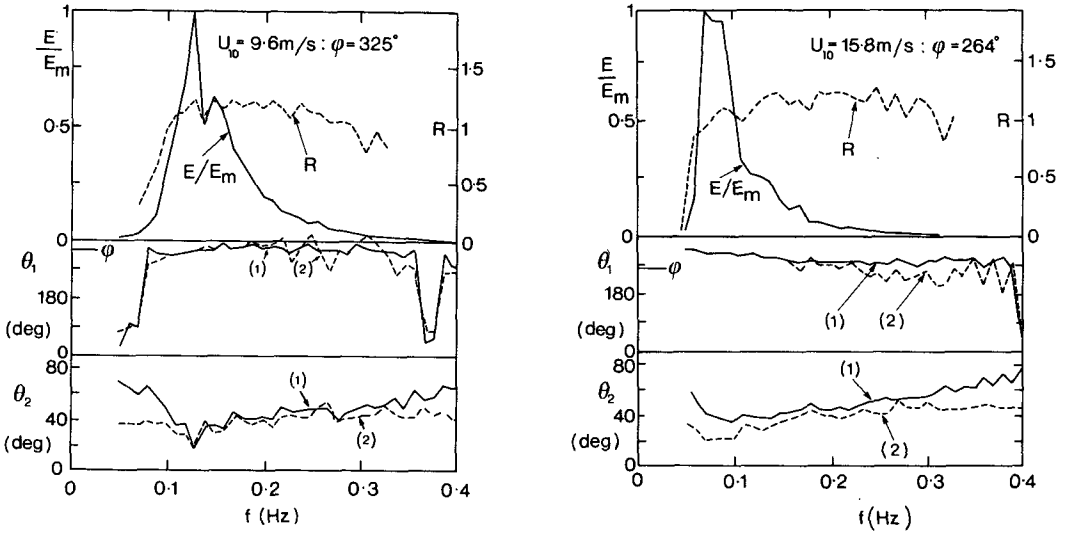

FIG. 3a. Directional spectrum obtained at 12 h, 6 July 1978. Upper diagram: normalized frequency spectrum [where $E_m = E(f_m)$] and check ratio, R. Middle diagram: wave directions from (1) first- and (2) second-order harmonics. Lower diagram: directional spread from first- and second-order harmonics.

FIG. 3b. As in 3a except obtained at 6 h, 17 May 1979.

TABLE 1. Summary of selected spectral observations for fully developed conditions at DB1. Wind speed and direction are denoted by U_{10} and ϕ. Other parameters are defined in the text. Directional information rejected for observations with asterisk.

Date			Time	U_{10}	ϕ	h_s	f_m					Meteorological
(yr	mo	d)	(h)	(m s^{-1})	(deg)	(m)	(Hz)	ν	α	γ	$\bar{e}\times 10^3$	changes
1978	6	29*	12	8.0	327	1.12	0.138	0.112	0.0024	1.68	1.84	
	7	4*	3	13.2	332	3.04	0.100	0.135	0.0054	1.51	1.83	
	7	5*	12	12.3	336	2.45	0.112	0.140	0.0055	1.05	1.58	
	7	6	12	9.6	325	1.80	0.128	0.125	0.0047	1.48	2.29	
	8	15	12	10.4	265	1.75	0.119	0.126	0.0040	1.34	1.57	d
1979	5	17	6	15.8	264	5.39	0.074	0.119	0.0052	0.80	2.80	df
	9	20	3	12.3	329	2.24	0.095	0.119	0.0028	0.86	1.32	df
1980	3	6*	3	15.1	251	4.26	0.078	0.120	0.0044	0.73	2.10	f
	3	7*	9	22.5	292	11.84	0.053	0.122	0.0067	0.70	3.29	
	5	20*	21	12.8	334	2.17	0.130	0.170	0.0073	1.39	1.06	df
	5	31	9	11.6	272	2.45	0.119	0.141	0.0064	1.27	1.99	df
	6	23	3	14.1	286	3.01	0.094	0.135	0.0054	0.62	1.38	
	7	9	6	10.7	337	1.82	0.138	0.150	0.0064	1.60	1.52	
	7	10	12	8.9	283	1.35	0.150	0.136	0.0057	1.34	1.75	
	7	13	18	10.7	266	2.00	0.120	0.131	0.0048	1.30	1.84	f
	7	19	6	9.9	241	1.68	0.130	0.132	0.0047	1.39	1.77	
	7	30	12	12.3	224	2.65	0.118	0.148	0.0061	2.14	1.85	df
	8	3	12	10.9	207	1.82	0.126	0.140	0.0058	1.00	1.41	f
	10	7*	12	17.6	311	7.69	0.072	0.129	0.0086	0.97	3.71	f
	10	9*	0	14.2	308	4.17	0.083	0.120	0.0050	0.91	2.57	
	10	22*	15	13.6	288	2.91	0.104	0.144	0.0062	0.88	1.49	d
	12	12	12	13.1	195	3.17	0.109	0.145	0.0068	1.38	2.05	f
	12	20	9	17.4	287	8.74	0.061	0.109	0.0067	0.96	5.01	f
1981	4	18	18	11.7	068	2.29	0.138	0.165	0.0078	1.76	1.68	
	5	12	12	10.9	290	1.54	0.151	0.167	0.0068	1.33	1.01	
	6	2*	9	10.6	203	2.10	0.128	0.139	0.0055	2.06	2.10	df
	6	8	15	14.4	225	3.09	0.101	0.148	0.0062	1.09	1.34	
	6	24	6	8.8	358	1.20	0.151	0.136	0.0040	1.79	1.44	f
	7	17	12	11.9	309	2.39	0.117	0.142	0.0069	1.32	1.71	
	7	22	12	12.4	312	2.48	0.119	0.150	0.0059	1.80	1.56	f
	7	23	12	13.3	327	3.20	0.103	0.140	0.0070	1.07	1.97	f
	9	14	6	11.3	203	2.32	0.123	0.142	0.0050	1.24	1.99	f
	11	28	6	13.6	305	3.41	0.090	0.125	0.0049	1.20	2.04	df

JONSWAP, Kahma (1981), and Donelan et al. (1985), we choose U_{10} as a suitable measure of U_∞. An alternative scaling using the friction velocity, which is influenced by the energy transfer from atmosphere to waves, was attempted, but we found no advantage in using this parameter.

If the total energy or variance in the wave record is e, similarity theory shows that the nondimensional energy $\bar{e} = eg^2/U_{10}^4$ and the nondimensional peak frequency ν should be constants at full development.

The work of Pierson and Moskowitz (1964) was based on wind measurements at a height of 19.5 m from ocean weather ships. We may convert these wind speeds to a height of 10 m using a factor of 0.93 (Pierson, 1977). With this conversion $\nu = 0.13$ and $\bar{e} = 3.64 \times 10^{-3}$ for values appropriate to a 10-m level. For the P–M spectral form we use the expression

$$E(f) = \alpha_{PM} g^2 (2\pi)^{-4} f^{-5} \exp\left[-\frac{5}{4}(f_m/f)^4\right] \quad (1)$$

where $\alpha_{PM} = 0.0081$ and $f_m = 0.13g/U_{10}$.

b. Observations of the frequency spectrum

Values of the nondimensional wave energy $\bar{e}$ are shown in Table 1. The energy in the P–M spectrum from 0.20 Hz to infinity is 10% of the total energy at 12.5 m s^{-1}. Truncation of our spectra at the same frequency implies that $\bar{e}$ can be underestimated by, at most, 10% for the majority of our observations. The mean value of $\bar{e}$ for all 33 wave spectra in our analysis was 1.97×10^{-3} with a standard deviation of 0.79×10^{-3}. The value of 3.64×10^{-3} for a P–M spectrum is significantly higher (with 98% confidence). Further, ordering the data with increasing wind speed shows that the three events with wind speeds in excess of 16 m s^{-1} are grouped separately, with a mean of 4.00×10^{-3}, while the rest have a mean of 1.76×10^{-3} with a standard deviation of 0.40×10^{-3}. There appears to be no systematic trend in $\bar{e}$ with U_{10} within the main group. (No trend was apparent in ν, α or γ as a function of U_{10}, either.)

The most likely reason for the difference between our estimate of $\bar{e} = 1.76 \times 10^{-3}$ for the majority of the

TABLE 2. Wind observations at OWS Romeo referred to wave arrival time at DB1.

Date			Time (event start)	U_{10}/ϕ	U_T/ϕ_T	U_{T-6}/ϕ_{T-6}	U_{T-12}/ϕ_{T-12}	U_{T-18}/ϕ_{T-18}
(yr	mo	d)	(h)	(at DB1)		(at OWS Romeo)		
1978	8	15	12	10.4/265	11.9/230	10.3/270	12.4/280	11.3/280
1979	5	7	6	15.8/264	15.0/310	15.5/310	15.5/310	15.5/310
1980	3	7	9	22.5/292	22.7/290	21.6/310	19.6/310	18.6/310
1980	7	19	6	9.9/241	8.2/250	10.8/240	10.8/240	9.3/250
1980	10	7	12	17.6/283	13.9/240	14.4/250	15.5/310	15.5/300
1980	10	9	0	14.2/308	13.9/310	13.9/290	13.4/320	12.4/300

spectra and the P–M value is that the waves had not reached the last stages of development. Another possibility is that the single-point estimates of wind speed at DB1 are not representative of the upwind fetch conditions: reducing the wind speed by about 20% will bring agreement with the P–M value of 3.64×10^{-3}. We are unable to resolve this discrepancy with the information available.

The spectra of the 33 individual spectra when scaled according to Kitaigorodskii are shown in Fig. 4 on logarithmic axes. For values of $U_{10}f/g$ greater than 0.13 the spectra are clearly well described by the similarity law. For values of $U_{10}f/g$ less than 0.13 there is more scatter in the observations, which may be due to the difficulties in determining the spectrum on the sharp forward face.

In the analysis of P–M, the wave spectra were grouped in wind speed intervals of 5 knots and then averaged. The nominal wind speed of each group was then adjusted to a new wind speed before the final estimation of the analytical form for the spectrum. Kitaigorodskii (1973, p. 128, footnote) has pointed out that this procedure is correct if the similarity law holds, but that a better procedure would be to form the nondimensional quantity Eg^3/U_{10}^5 for each individual spectrum and then average these quantities over wind speed classes. We have used this method and grouped our results into six classes. For wind speeds between 10 and 16 m s^{-1} an interval of 2 m s^{-1} separates the classes. Only one observation is available at a wind speed greater than 20 m s^{-1} and this is given as class 6 (see Table 3).

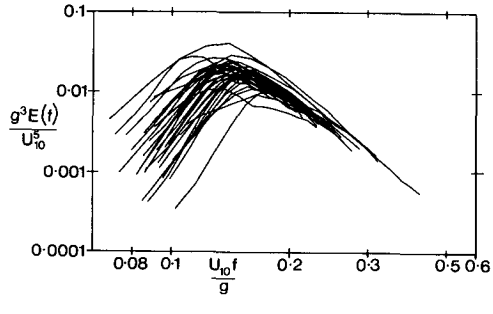

FIG. 4. Scaled frequency spectra for all observations.

Figure 5 shows the results on a linear axes plot and compares the averaged observed spectra with P–M form. The four classes with wind speeds less than 16 m s^{-1} are consistently below the P–M form, especially for frequencies above the spectral peak. This is confirmed by the low values of α compared with $\alpha_{PM} = 0.0081$ (Table 3). The two classes with the highest wind speeds have peak values close to the P–M form.

It is also possible to scale the spectra with respect to peak frequency, f_m. This has the advantage that cumulative effects of the fetch are represented, unlike the single point nature of the wind speed scaling. However, it has the disadvantage that each peak frequency is subject to a large sampling error (see Pierson, 1977). Figure 6 shows the result of using this scaling and confirms that the observed spectra generally lie below the P–M spectrum; the variation of the peak values is less than that for the wind speed scaling in Fig. 5.

6. The directional spectra

The characteristic of the directional spectrum that we are particularly interested in is the directional spread. For a unimodal directional distribution of the form $G(\theta) \sim \cos^{2s}\frac{1}{2}(\theta - \theta_1)$, we can obtain two estimates of s: from the first- and second-order angular harmonics (see the Appendix). Figure 3b and other analyses show that for some measurements the values of s_1 are much less than s_2. This appears to be an inherent feature of many surface following wave buoys, including the free drifting IOS pitch–roll buoy (Hasselmann et al., 1980) and the moored WAVEC buoy (van der Vlugt, 1982). We first discuss possible reasons for the discrepancy between s_1 and s_2.

TABLE 3. Estimates of the JONSWAP parameters (γ, α) for six wind speed classes. N is the number of observations in each class.

Class	U_{10} (m s^{-1})	N	γ	α
1	≤10	5	1.01	0.0040
2	10–12	10	1.07	0.0056
3	12–14	10	1.05	0.0064
4	14–16	5	1.00	0.0042
5	16–20	2	0.97	0.0077
6	>20	1	0.70	0.0067

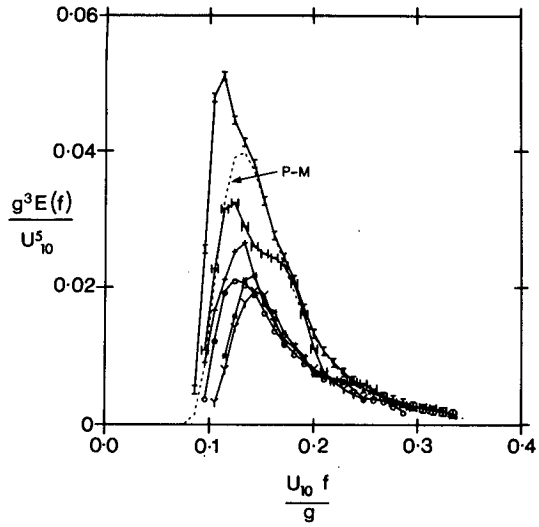

FIG. 5. Averaged scaled frequency spectra for six windspeed classes compared with the Pierson–Moskowitz spectrum. Key: (+) $U_{10} < 10$ m s^{-1}; (*) $10 \leq U_{10} < 12$ m s^{-1}; (Y) $12 \leq U_{10} < 14$ m s^{-1}; (O) $14 \leq U_{10} < 16$ m s^{-1}; (I) $16 \leq U_{10} < 20$ m s^{-1}; (H) $U_{10} \geq 20$ m s^{-1}.

a. Bimodality

Bimodality in the directional distribution can produce different values of the spread parameters s_1 and s_2. For simplicity, consider a simple bimodal system comprising two Gaussian distributions with predominant directions ϕ_1 and ϕ_2, namely

$$NG(\theta) = (1 - R_1)\exp[-0.25s(\theta - \phi_1)^2] + R_1 \exp[-0.25s(\theta - \phi_2)^2]$$

where R_1 is the proportion of the total energy propagating in the direction ϕ_2. The normalizing factor is $N = (s/4\pi)^{1/2}$. The rms spread of each distribution is $(2/s)^{1/2}$.

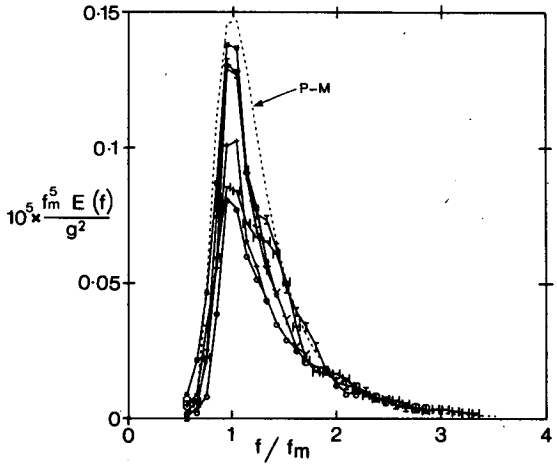

FIG. 6. Frequency spectra scaled with peak frequency, f_m, compared with the Pierson–Moskowitz spectrum. Key as for Fig. 5.

We take a value of $s = 10$ as being typical of our data. The four angular harmonics, and hence s_1 and s_2, were then computed for values of $R = 0.05$, 0.1, 0.5 and as a function of the angular separation $\Delta\phi = \phi_1 - \phi_2$ (Fig. 7). As $\Delta\phi$ increases, both s_1 and s_2 decrease at about the same rate until $\Delta\phi$ reaches 90°. For angular separations exceeding 90° there is a large difference between s_1 and s_2.

Bimodality does not appear to be the cause for the large differences in s_1 and s_2 in our measurements, however, since the meteorological conditions were carefully selected to exclude any wind situations which could generate waves from widely separated directions. The nearest coastline was too distant to produce any significant reflected wave energy.

b. Data simulations

We have investigated the influence of noise in the slope measurements on the directional wave analysis using simulation techniques following the principles given by Tucker et al. (1984).

Consider a time series for wave elevation η given by

$$\eta(\mathbf{x}, t) = \sum_{\mathbf{k}_i} \sum_{\omega_j} [a_{ij}\cos(\mathbf{k}_j \cdot \mathbf{x} - \omega_i t) + b_{ij}\sin(\mathbf{k}_j \cdot \mathbf{x} - \omega_i t)]$$

where $\mathbf{k}_j$ and ω_i are the wavenumber and angular frequency of the jth and ith bands. The variables a_{ij} and b_{ij} are coefficients estimated from the spectrum which is to be simulated. Assuming a linear wave field, $\mathbf{k}$ and ω are related through the dispersion relation, thus reducing the summation to

$$\eta(\mathbf{x}, t) = \sum_{\theta_i} \sum_{\omega_j} [a_{ij}\cos(\mathbf{k}_{ij} \cdot \mathbf{x} - \omega_j t) + b_{ij}\sin(\mathbf{k}_{ij} \cdot \mathbf{x} - \omega_j t)]$$

where $\mathbf{k}_{ij}$ indicates that the wavenumber is specified by the direction θ_i and frequency ω_j.

The expressions η, a_{ij} and b_{ij} are Gaussian-distributed, the latter two with variances given by the frequency–direction spectrum, $E(\omega, \theta)$. If $\Delta\theta_i$, $\Delta\omega_j$ are the bandwidths of the ith directional and jth frequency band, then the variance of a_{ij} and b_{ij} is $E(\omega_j, \theta_i)\Delta\theta_i\Delta\omega_j$. A Gaussian random number generator with this vari-

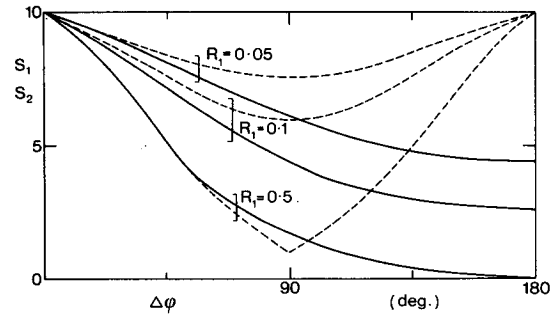

FIG. 7. Spread parameters s_1 (solid line) and s_2 (dashed line) for bimodal Gaussian distributions. R_1 gives the proportion of energies in the distributions. $\Delta\phi$ is the angular separation.

ance provides values of a_{ij} and b_{ij}. An inverse Fourier Transform then generates the time series for η.

Since the time series for a buoy is a point measurement, we set $x = 0$, thus

$$\eta(t) = \sum_{\theta_i} \sum_{\omega_j} [a_{ij} \cos(\omega_j t) - b_{ij} \sin(\omega_j t)].$$

Using the same values of a_{ij} and b_{ij}, we have the acceleration signal

$$\ddot{\eta}(t) = \sum_{\theta_i} \sum_{\omega_j} -\omega^2 [a_{ij} \cos(\omega_j t) - b_{ij} \sin(\omega_j t)],$$

and the slope signals

$$\eta_x(t) = \sum_{\theta_i} \sum_{\omega_j} [-a_{ij} k_{ijx} \sin(\omega_j t) - b_{ij} k_{ijx} \cos(\omega_j t)]$$

$$\eta_y(t) = \sum_{\theta_i} \sum_{\omega_j} [-a_{ij} k_{ijy} \sin(\omega_j t) - b_{ij} k_{ijy} \cos(\omega_j t)]$$

where k_{ijx} and k_{ijy} are the wave number components in the x and y directions, respectively.

For the spectrum to be simulated we have chosen a P-M form with variance 1 m^2 and directional distribution $G(\theta) \sim \cos^6\theta$, $|\theta| \leq \pi/2$. Noise was introduced into the slope signals. This was uniformly distributed on the range $[-c\sigma, c\sigma]$ where σ was the standard deviation of the slope and c was varied between 0 and 0.5. The directional wave spectrum and associated parameters were then estimated from the simulated time series using standard computer programs. Table 4 shows the effect of adding an increasing amount of noise to the slope signals which, without noise, had an initial variance of 0.0117 radians^2. The value of A_1 (see the Appendix) decreases with increasing noise; this can also be seen by considering the expression for A_1, in which the numerator is less affected by noise than the denominator. As s_1 is very sensitive to small changes in A_1, there are accordingly large changes in s_1, which is then also biased low. However, an increase in noise in the slope signals produces a small change in A_2. This in turn has a minor effect on s_2, as s_2 is not very sensitive to variations in A_2. (The pitch and roll transfer functions cancel out in the expressions for A_2 and B_2.) The total slope variance is slightly increased by the addition of noise. We therefore suggest that low values of s_1 may be due to noise present in the slope signals and that s_2 is a more reliable parameter describing the directional spread.

TABLE 4. Results from numerical simulations of directional spectra with noise added to the slope signals. A_1 and A_2 are the angular harmonics; s_1 and s_2 are estimates of the spread.

Noise level, c	Total slope variance σ^2 (rad^2)	A_1	A_2	s_1	s_2
0	0.0117	0.930	0.744	14.4	14.5
0.1	0.0118	0.925	0.743	14.3	14.8
0.3	0.0119	0.920	0.744	12.4	14.4
0.5	0.0119	0.905	0.748	10.2	15.1

c. *Alternative analysis procedure*

As an alternative method to the conventional analysis method of Longuet-Higgins et al. (1963) we have used the variational technique of Long and Hasselmann (1979), which is capable of recovering bimodal directional distributions (Lawson and Long, 1983). Calculations were made for selected directional spectra where there were large differences between s_1 and s_2. No assumption is made in the variational method for the form of the directional distribution. We then calculated the rms directional spread from the computed spectrum and converted this to an equivalent value of s (s_v as included in Table 5). (In some frequency bands the variational method gave a small secondary peak; this has not been included in the calculation.) The value of s_v from the variational method agrees well with s_2 estimated from the second harmonics and confirms the view that s_2 is a suitable parameter for describing the directional spread.

d. *Results for the directional spread*

Estimates of s_2 for all cases where these are valid directional spectra are shown in Fig. 8 as a function of f/f_m. Values of s_2 below the spectral peak are not shown since they were very scattered. For each spectrum a least-squares fit was made to the data for the same classes used in the analysis of the frequency spectrum using a function of the form $s_2 = g(f/f_m)^h$. Estimates of g and h, when the correlation coefficient from the fit was greater than 0.5, are shown in Table 6. There does not appear to be any systematic variation of g and h with wind speed. Figure 8 also compares the results with the expression given by Hasselmann et al. (1980), namely

$$s = 9.77(f/f_m)^{-2.33}, \quad f \geq f_m. \tag{3}$$

The peak values of s_2 at $f = f_m$ are close to Eq. (3) but the decrease with f/f_m is slower. There is no evidence in our results of a narrower directional spread above the spectral peak as suggested by Komen et al. (1984); this may, however, be due to the limited directional resolution available from surface following buoys.

For comparison we also show the results for s_1 in Fig. 9. The values of s_1 lie below the relation given by Hasselmann et al. (1980) and, as discussed earlier, are considered less reliable than s_2. The least-squares fit to the data above f_m has a slope of -1.04 which is different from the relation given by Hasselmann et al. (1980) but has the same form of frequency dependence as s_2.

7. Conclusions

The frequency spectra for fully developed conditions are described by the similarity law of Kitaigorodskii

TABLE 5. Comparisons of the spread parameters s_1 and s_2 with results s_v from a variational method.

f (Hz)	1200 h 15 Aug 1978			0600 h 14 Sep 1981		
	s_v	s_1	s_2	s_v	s_1	s_2
0.089	11.8	4.0	22.5	2.3	2.7	2.4
0.099	15.6	1.8	17.5	4.2	5.0	4.8
0.109	10.0	4.0	10.7	7.3	5.2	7.0
0.119	13.5	6.3	13.9	8.7	7.8	8.3
0.129	11.2	4.1	11.8	14.2	8.4	13.7
0.139	7.9	2.8	8.6	7.9	7.2	7.8
0.149	6.9	3.2	7.4	7.6	4.9	7.3

TABLE 6. Estimates of the least-squares fit for the parameter s_2 for wind speed classes. N is the number of observations in each class.

Class	U_{10} m s^{-1}	N	g	h
1	≤10	4	10.6	−1.62
2	10–12	9	8.2	−1.26
3	12–14	6	9.3	−1.18
4	14–16	3	11.3	−1.24

(1962, Chap. 6) for frequencies above the spectral peak. Below the peak of the wave spectrum there is more scatter in the observations which may be due to difficulties in determining the shape of the spectrum on the steep forward face.

The observed wave spectra were grouped into six classes of wind speed with an interval of 2 m s^{-1} for those classes lying between 10 and 16 m s^{-1}. The spectra were first made nondimensional by forming the quantity Eg^3/U_{10}^5 before averaging over wind speed classes as advocated by Kitaigorodskii (1973, p. 128, footnote). For the lower wind speed classes, with U_{10} less than 16 m s^{-1}, we find the averaged spectrum lies consistently below the Pierson–Moskowitz spectrum, while for higher wind speeds the spectra in the region of the peak have similar values to the P–M spectrum. Despite quite comprehensive selection criteria the most likely reason for the difference between our observed wave spectra and the Pierson–Moskowitz form is that in the majority of our observations the waves had not reached the last stages of development. Another possibility is that single-point estimates of wind speed at DB1 are not representative of the upwind fetch conditions. We are unable to resolve this discrepancy with the information available.

We have studied the directional spread by considering the two estimates s_1 and s_2 of the exponent of a cosine power law directional distribution obtained from the first- and second-order harmonics of this distribution. Values of s_1 were found to be much less than those of s_2. We account for this difference as being due to noise in the slope signals, as confirmed by numerical simulations. Bimodality in the directional distribution is not considered to be the cause of this difference. The variational method of Long and Hasselmann (1979) was also used to estimate the directional spread and gave values close to those for s_2. The parameter s_2 was therefore considered to be more reliable than s_1.

Estimates of s_2 as a function of wave frequency in relation to peak frequency differ from the expression given for fetch-limited waves. Although the peak value of s_2 at $f = f_m$ is close to that in the formulation of Hasselmann et al. (1980), the decrease with f/f_m is less rapid. There does not appear to be evidence for a narrower directional spread above the spectral peak as found in the theoretical work of Komen et al. (1984). Further studies using systems with better angular resolution than surface following wave buoys are needed to study this aspect.

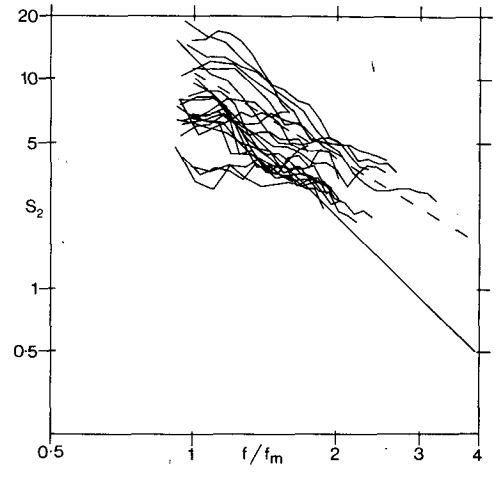

FIG. 8. Spread parameter s_2 for frequencies greater than f_m. The continuous line is from Hasselmann et al. (1980). The dashed line is the least-squares fit to all data (g = 10.3, h = −1.41).

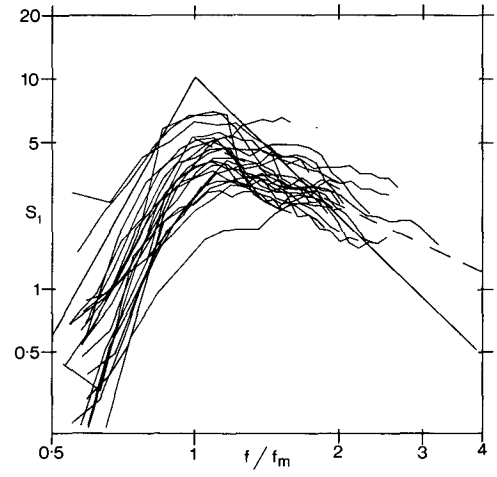

FIG. 9. As in Fig. 8 except for spread parameter s_1 as a function of f/f_m.

Acknowledgments. The authors are grateful to the Oceanographic Committee of the United Kingdom Offshore Operators Association for permission to use wave and wind data from DB1 in this study. We thank Dr. A. R. Tabor of the Marine Information and Advisory Service of IOS for his help in accessing these data and the referees for their helpful remarks. A.K.L. would like to thank the New Zealand Research Advisory Council for sponsoring a period of study leave at the IOS.

APPENDIX

Determination of the Directional Spectrum

The pitch, roll and compass channels are used to derive the two components of surface slope with respect to N–E axes. Let subscripts 2 and 3 denote the components of surface slope in the north and east directions, respectively. Let subscript 1 refer to the series for vertical displacement taking into account the transfer function resulting from electronic double integration. Then it can be shown that the six cross spectra derived from the wave buoy system are given by

$$C_{11}(f) = \int_0^{2\pi} F(f,\theta)d\theta$$

$$C_{22}(f) = \int_0^{2\pi} k^2 \cos^2\theta F(f,\theta)d\theta$$

$$C_{33}(f) = \int_0^{2\pi} k^2 \sin^2\theta F(f,\theta)d\theta$$

$$Q_{12}(f) = \int_0^{2\pi} k \cos\theta F(f,\theta)d\theta$$

$$Q_{13}(f) = \int_0^{2\pi} k \sin\theta F(f,\theta)d\theta$$

$$C_{23}(f) = \int_0^{2\pi} k^2 \sin\theta \cos\theta F(f,\theta)d\theta, \qquad \text{(A1)}$$

where C_{ij} and Q_{ij} are the co- and quadrature spectra of series i with j. The $F(f, \theta)$ is the directional wave spectrum with respect to frequency f and direction of propagation θ. The variable k is the wavenumber. Only five of the cross spectra are independent. This allows estimation of the five Fourier coefficients in the expansion of $F(f, \theta)$, namely,

$$a_n + ib_n = \frac{1}{\pi}\int_0^{2\pi} e^{in\theta} F(f,\theta)d\theta, \quad n = 0, 1, 2. \qquad \text{(A2)}$$

In the calculations it is convenient to compute the normalized angular harmonics $A_1 = a_1/a_0$, etc., where πa_0 is the one-dimensional spectrum obtained by integrating $F(f, \theta)$ over all directions. Thus

$$A_1 = \frac{Q_{12}}{[C_{11}(C_{22}+C_{33})]^{1/2}}, \quad B_1 = \frac{Q_{13}}{[C_{11}(C_{22}+C_{33})]^{1/2}},$$

$$A_2 = \frac{C_{22}-C_{33}}{C_{22}+C_{33}}, \quad B_2 = \frac{2C_{23}}{C_{22}+C_{33}}. \qquad \text{(A3)}$$

In the preceding equations we make use of the relation

$$[C_{11}/(C_{22}+C_{33})] = 1/k^2.$$

Assuming the dispersion relation for waves of small amplitude in deep water, $(2\pi f)^2 = gk$, the quantity

$$R = (2\pi f)^2/g \cdot [C_{11}/(C_{22}+C_{33})]^{1/2}$$

should be unity. Thus, R provides a check on the correct functioning of the wave buoy system and on the analysis.

If the directional distribution is unimodal and of the form $G(\theta) \sim \cos^{2s}\frac{1}{2}(\theta - \theta_1)$, we may derive the following parameters:

(i) First-order angular harmonics

mean wave direction:

$$\theta_1 = \arctan(B_1/A_1),$$

spread parameter:

$$s_1 = C_1/(1 - C_1) \quad \text{where} \quad C_1^2 = A_1^2 + B_1^2.$$

(ii) Second-order angular harmonics

mean wave direction:

$$\theta_{12} = \frac{1}{2}\arctan(B_2/A_2),$$

spread parameter:

$$s_2 = [(1 + 3C_2 + (1 + 14C_2 + C_2^2)^{1/2}]/[2(1 - C_2)]$$

where

$$C_2^2 = A_2^2 + B_2^2.$$

We also define a parameter $\theta_2 = [2/(s + 1)]^{1/2}$, where s can be determined from the first- or second-order angular harmonics. For a narrow directional distribution θ_2 is the rms spread about the mean wave direction.

All wave directions are defined as those directions *from* which the waves are coming.

REFERENCES

Cartwright, D. E., 1963: The use of directional spectra in studying the output of a wave recorder on a moving ship. *Ocean Wave Spectra,* Prentice-Hall, 203–218.

Clayson, C. H., and J. A. Ewing, 1977: The buoy as a directional wave sensor. Institute of Oceanographic Sciences, Rep. No. 44. [Contribution to U.K. Data Buoy (DB1) Symposium, Wormley, 23 Nov. 1976.]

Donelan, M. A., J. Hamilton and W. H. Hui, 1985: Directional spectra of wind-generated waves. *Phil. Trans. Roy. Soc. London,* **A315,** 509–562.

Freathy, P. E., A. G. Hooper and H. W. MacDonald, 1982: Wind and wave directional data obtained from DB1 in the SW approaches to the United Kingdom. *Int. Conf. on Wave and Wind Directionality,* Paris, Editions Technip, 33–44.

Hasselmann, D. E., M. Dunckel and J. A. Ewing, 1980: Directional spectra observed during JONSWAP 1973. *J. Phys. Oceanogr.,* **10,** 1264–1280.

Hasselmann, K., T. P. Barnett, E. Bouws, H. Carlson, D. E. Cartwright, K. Enke, J. A. Ewing, H. Gienapp, D. E. Hasselmann, P. Kruseman, A. Meerburg, P. Muller, D. J. Olbers, K. Richter, W. Sell and H. Walden, 1973: Measurements of wind-wave growth and swell decay during the Joint North Sea Wave Project (JONSWAP). *Dtsch. Hydrogr. Z.,* **A8**(12).

——, D. B. Ross, P. Muller and W. Sell, 1976: A parametric wave prediction model. *J. Phys. Oceanogr.,* **6,** 200–228.

Kahma, K. K., 1981: A study of the growth of the wave spectrum with fetch. *J. Phys. Oceanogr.,* **11,** 1503–1515.

Kim, W. D., 1966: On a free-floating ship in waves. *J. Ship Res.,* **10,** 182–200.

Kitaigorodskii, S. A., 1962: Applications of the theory of similarity to the analysis of wind-generated wave motion as a stochastic process. *Izv. Akad. Nauk SSSR, Ser. Geogr. Geofiz.,* **1,** 105–117.

——, 1973: *The Physics of Air–Sea Interaction.* Israel Program for Scientific Translations, Jerusalem, 237 pp.

Komen, G. J., S. Hasselmann and K. Hasselmann, 1984: On the existence of a fully developed wind-sea spectrum. *J. Phys. Oceanogr.,* **14,** 1271–1285.

Lawson, L. M., and R. B. Long, 1983: Multimodal properties of the surface-wave field observed with pitch-roll buoys during GATE. *J. Phys. Oceanogr.,* **13,** 474–486.

Long, R. B., and K. Hasselmann, 1979: A variational technique for extracting directional spectra from multicomponent wave data. *J. Phys. Oceanogr.,* **9,** 373–381.

Longuet-Higgins, M. S., D. E. Cartwright and N. D. Smith, 1963: Observations of the directional spectrum of sea waves using the motions of a floating buoy. *Ocean Wave Spectra,* Prentice-Hall, 111–136.

Müller, P., 1976: Parameterization of one-dimensional wind-wave spectra and their dependence on the state of development. No. 31, *Hamburger Geophys. Einzelschriften,* Geophysikalische Institut University of Hamburg.

Phillips, O. M., 1958: The equilibrium range in the spectrum of wind-generated waves. *J. Fluid Mech.,* **4,** 426–434.

Pierson, W. J., 1977: Comments on "A parametric wave prediction model". *J. Phys. Oceanogr.,* **7,** 127–134.

——, and L. Moskowitz, 1964: A proposed spectral form for fully developed wind seas based on the similarity theory of S. A. Kitaigorodskii. *J. Geophys. Res.,* **69,** 5181–5190.

Tucker, M. J., P. G. Challenor and D. J. T. Carter, 1984: Numerical simulation of a random sea: A common error and its effect upon wave group statistics. *Appl. Ocean Res.,* **6,** 118–122.

van der Vlugt, A. J. M., 1982: The WAVEC buoy for routinely measuring the direction of sea waves. *Int. Conf. on Wave and Wind Directionality,* Paris, Editions Technip, 131–141.

Wu, J., 1982: Wind stress coefficients over sea surface from breeze to hurricane. *J. Geophys. Res.,* **87,** 9704–9706.